REPORT No. 808

A METHOD FOR THE CALCULATION OF EXTERNAL LIFT, MOMENT, AND PRESSURE DRAG OF SLENDER OPEN-NOSE BODIES OF REVOLUTION AT SUPERSONIC SPEEDS

By Clinton E. Brown and Hermon M. Parker

SUMMARY

An approximate method is presented for the calculation of the external lift, moment, and pressure drag of slender open-nose bodies of revolution at supersonic speeds. The lift, moment, and pressure drag of a typical ram-jet body shape are calculated at Mach numbers of 1.45, 1.60, 1.75, and 3.00; and the lift and moment results are compared with available experimental data. The agreement of the calculated lift and moment data with the experimental data is excellent. The pressure-drag comparison was not presented because of the uncertainty of the amount of skin-friction drag present in the experimental results. It was found that the lift coefficient definitely increased with increasing Mach number, whereas the moment coefficient taken about the midpoint of the body and the drag coefficient decreased with increasing Mach number. The manner in which the method may be applied to slender bodies of revolution with annular air inlets is shown. The excellent agreement of the calculated lift and moment results with experimental data indicates that the approximate method may be reliably used for obtaining the aerodynamic characteristics of slender bodies that are required for efficient supersonic flight.

INTRODUCTION

Current proposals for the design of aircraft capable of sustained flight at supersonic speeds and utilizing the ram jet as a method of propulsion have established the importance of knowing the aerodynamic characteristics of slender open-nose bodies of revolution at speeds greater than the speed of sound. The lack of theoretical treatments and experimental data emphasizes the need for theoretical investigation of this problem to serve as a guide for future work and as a check on the reasonableness of current and future experimental results.

The small-perturbation approximation was used in reference 1 to deduce the wave drag and in reference 2 to obtain the lift and moment of slender pointed-nose bodies of revolution. No fundamental analysis is known to have been made, however, of the characteristics of a slender open-nose body shape, such as that required by ram-jet propelled craft. The peculiarity of the problem, from general considerations of similarity, is that the flow pattern is two dimensional at the lip of the nose and approaches the three-dimensional pattern farther along the body. The present work extends the method of references 1 and 2 to apply to these slender open-nose bodies of revolution with supersonic flow into the nose. The result is a fairly simple method of numerical integration of the differential equation of the flow. As an illustration, the pressure distribution, wave drag, lift, and moment are calculated at Mach numbers of 1.45, 1.60, 1.75, and 3.00 for a typical ram-jet airplane body shape; and the lift and moment results are compared with the experimental data. It should be pointed out that the accuracy of the method, which assumes potential supersonic flow throughout the field and also assumes small disturbances, depends on the surface angles of the body and the Mach number. The error increases with either increasing Mach number or increasing surface angles.

SYMBOLS

x, r, θ	cylindrical coordinates
X	distance along x-axis measured from nose of body
l	length of body
R	radius of body
β	Mach angle $\left(\sin^{-1}\frac{1}{M}\right)$
$B=\sqrt{M^2-1}$	
$\phi\ (x, r, \theta)$	perturbation potential
$\phi_1\ (x, r)$	perturbation potential for axial flow
$\phi_2\ (x, r, \theta)$	perturbation potential for cross flow
v_x	axial velocity increment $\left(\frac{\partial\phi}{\partial x}\right)$
v_r	radial velocity increment $\left(\frac{\partial\phi}{\partial r}\right)$
V	velocity in undisturbed stream
a	velocity of sound in undisturbed stream
M	Mach number in undisturbed stream (V/a)
ρ	density in undisturbed stream
Δp	incremental surface pressure due to angle of attack
p_l	local pressure
p	pressure in undisturbed stream
γ	ratio of specific heats of air (1.4)
α	angle of attack, radians (except where otherwise noted)
δ	angle between surface of body and x-axis

C_L lift coefficient $\left(\text{Lift}/\frac{\rho}{2}V^2\pi R_N^2\right)$

C_D drag coefficient $\left(\text{Drag}/\frac{\rho}{2}V^2\pi R_N^2\right)$

C_m moment coefficient $\left(\text{Moment}/\frac{\rho}{2}V^2\pi R_N^2 l\right)$

u variable of integration

$\xi=x-Br\cosh u$

$j_i=x_i-BR_i$

$T_i^n=\frac{x_n-j_i}{BR_n}$

$A_i=f'(\xi)_i$

SUBSCRIPTS AND SUPERSCRIPTS

N refers to nose

n refers to nth integration station, summation variable

i refers to ith integration station, summation variable

deg in degrees

MATHEMATICAL ANALYSIS

POINTED BODIES OF REVOLUTION

The linearized equation of motion of a nonviscous compressible fluid may be written for a cylindrical coordinate system:

$$\frac{\partial^2\phi}{\partial r^2}+\frac{1}{r}\frac{\partial\phi}{\partial r}+\frac{1}{r^2}\frac{\partial^2\phi}{\partial\theta^2}=(M^2-1)\frac{\partial^2\phi}{\partial x^2} \tag{1}$$

where ϕ is the potential function assumed to represent the effect of a small disturbance set up by the slender bodies being considered. The problem is to find a solution of equation (1) that will satisfy the known boundary conditions at the surface of the body. A general solution of the differential equation (1), when $M>1$, for diverging waves has been found by Lamb (reference 3) to be, with a slight change in notation,

$$\phi=\sum_s Q_s r^s\cos s\theta+P_s r^s\sin s\theta$$

where

$$\left.\begin{aligned}Q_s&=\left(\frac{\partial}{r\partial r}\right)^s Q_0\\ P_s&=\left(\frac{\partial}{r\partial r}\right)^s P_0\end{aligned}\right\} \tag{2}$$

and

$$Q_0=\int_0^\infty f(x-Br\cosh u)du$$

$$P_0=\int_0^\infty g(x-Br\cosh u)du$$

where

$$B=\sqrt{M^2-1}$$

The part of Lamb's general solution corresponding to converging waves does not apply to the present problem because all disturbances originate on the body and diverge into the flow field investigated. Von Kármán and Moore have investigated the problem of the resistance of projectiles and cones (reference 1) and have found a solution for the case of axial symmetry

$$\phi=-\int_0^\infty f(x-Br\cosh u)du \tag{3}$$

that can be seen to be a special case of the general solution with $s=0$. In their analysis the body, in this case a sharp-nose projectile, was represented by a distribution of sources along the x-axis starting at $x=0$, the nose of the body. By a numerical method of integration, it became possible to write the equations for the velocity increments v_r and v_x,

$$v_{r_n}=-B\sum_{i=1}^{n}A_i\left[\sqrt{(T_i^n)^2-1}-\sqrt{(T_{i-1}^n)^2-1}\right] \tag{4}$$

$$v_{x_n}=\sum_{i=1}^{n}A_i[\cosh^{-1}(T_i^n)-\cosh^{-1}(T_{i-1}^n)] \tag{5}$$

where

$$T_i^n=\frac{x_n-j_i}{BR_n}$$

and

$$j_i=x_i-BR_i$$

$$A_i=f'(\xi)_i$$

with the boundary conditions

$$\frac{v_r}{V+v_x}=\frac{dr}{dx} \tag{6}$$

These three equations in three unknowns (A_n, v_{r_n}, v_{x_n}) were solved at each station on the body for v_r and v_x. The pressures were then found from the Bernoulli equation in the form:

$$\frac{p_i}{p}=\left[1+\frac{\gamma-1}{2}\left(-2M\frac{v_x}{a}-\frac{v_x^2+v_r^2}{a^2}\right)\right]^{\frac{\gamma}{\gamma-1}} \tag{7}$$

Ferrari (reference 4) and Tsien (reference 2) have independently found solutions for the case of pointed bodies of revolution at small angles of attack. Their solutions showed that the potential could be expressed in two terms: the first, from equation (3),

$$\phi_1=-\int_0^\infty f_1(x-Br\cosh u)du$$

is the solution for the pure axial flow already described; and the second

$$\phi_2=-B\cos\theta\int_0^\infty f_2(x-Br\cosh u)\cosh u\,du \tag{8}$$

represents the cross-flow potential of an arbitrary distribution of doublets along the axis of the body starting at the nose of the cone or projectile. The form of equation (8) is that the cross flow is from the direction $\theta=0$, as shown in figure 1.

By neglecting the small effect of the axial flow on the lifting pressures, Tsien obtained for the pointed projectile of arbitrary shape the equations:

$$C_L=\frac{2\alpha}{B}\sum_n \frac{x_{n+1}-x_n}{R_{base}}\frac{R_{n+1}+R_n}{R_{base}}\sum_{i=0}^{n}\frac{B^2K_i}{2\alpha V}\left[\sqrt{(T_{i-1}{}^n)^2-1}-\sqrt{(T_i{}^n)^2-1}\right] \tag{9}$$

$$C_m=-\frac{2\alpha}{Bl}\sum_n\left[\frac{x_{n+1}+2x_n}{3}+\left(\frac{x_{n+1}-x_n}{\cdot 3}\frac{R_{n+1}}{R_{n+1}+R_n}\right)\right]\left(\frac{x_{n+1}-x_n}{R_{base}}\frac{R_{n+1}+R_n}{R_{base}}\right)\sum_{i=0}^{n}\frac{B^2K_i}{2\alpha V}\left[\sqrt{(T_{i-1}{}^n)^2-1}-\sqrt{(T_i{}^n)^2-1}\right] \tag{10}$$

$$1=\sum_{i=1}^{n}\frac{B^2K_i}{2\alpha V}\left[\cosh^{-1}(T_{i-1}{}^n)-\cosh^{-1}(T_i{}^n)+(T_{i-1}{}^n)\sqrt{(T_{i-1}{}^n)^2-1}-T_i{}^n\sqrt{(T_i{}^n)^2-1}\right] \tag{11}$$

The values K_i in these equations are assumed to be constants for each interval of the step-by-step process. The moment coefficient of equation (10) is assumed positive for nosing-up moments, these moments being taken about the nose.

OPEN-NOSE BODIES

The flow conditions over an open-nose body differ from those of pointed bodies in that, for finite angles of the nose lip, the flow is two dimensional at the lip. This problem was not considered in references 1, 2, and 4 and the general solution should therefore be examined to determine its applicability to this special case. Lamb has shown (reference 3) that a sufficient requirement for the existence of the general solution to the differential equation of motion (reference 1) is that $f(x-Br\cosh u)$ be zero for all values of the argument less than some arbitrary limiting value. The determination of $f(x-Br\cosh u)$ such that the boundary conditions at the open-nose body are satisfied assures the fulfillment of this general requirement. For the usual case of supersonic flow into the nose, the boundary condition requires the surface of the body to be a continuation of a cylindrical stream surface of radius R_N in the undisturbed flow ahead of the body as shown in figure 2. The perturbation potentials, equations (3) and (8), therefore must be zero at the cylindrical stream surface ahead of the body. Substituting $\xi=x-Br\cosh u$ in equations (3) and (8) gives

$$\phi_1=-\int_{-\infty}^{x-Br}\frac{f_1(\xi)d\xi}{\sqrt{(x-\xi)^2-B^2r^2}} \tag{12}$$

and

$$\phi_2=-\frac{\cos\theta}{r}\int_{-\infty}^{x-Br}\frac{f_2(\xi)(x-\xi)d\xi}{\sqrt{(x-\xi)^2-B^2r^2}} \tag{13}$$

It is obvious that the boundary conditions are satisfied by letting $f_1(\xi)=f_2(\xi)=0$ for all values of $\xi<x_0-BR_0$, where the point (x_0, R_0) is at the lip of the open-nose body. It then remains to determine $f_1(\xi)$ and $f_2(\xi)$ for $\xi>x_0-BR_0$ so that the body surface is a continuation of this stream surface. From physical considerations, $f_1(\xi)$ and $f_2(\xi)$ may be regarded as an axial distribution of sources and doublets, respectively, where ξ is measured along the x-axis. Because the effect of a source or doublet can be felt only along or behind its Mach cone, the source distribution must begin a distance BR_0 ahead of the nose. This point is chosen for the origin of the coordinate system. (See fig. 1.) It must be emphasized that the source and doublet distribution determined by satisfying the boundary conditions at the stream and body surfaces shown in figure 2 does not represent correctly the flow inside that stream surface. This result corresponds to the physical fact that the actual supersonic flow into the nose does not affect the flow external to the body. The basic assumptions of potential flow and small disturbances are valid provided the slope of the body surface is small. Actually, for finite angles of the nose lip, a nonconical shock wave is formed that causes a loss in total pressure and produces rotation in the field.

Numerical integration of equation (12), with constant values of $f_1'(\xi)$ assumed over the integration intervals, results in the same expressions for v_{r_n} and v_{x_n} as those obtained by Von Kármán and Moore (equations (4) and (5)) These constant values of $f_1'(\xi)$ are determined by satisfying the boundary condition:

$$\frac{v_r}{V+v_x}=\tan\delta_n \tag{14}$$

where $\tan\delta_n$ is the slope of surface of the body at the nth interval of integration.

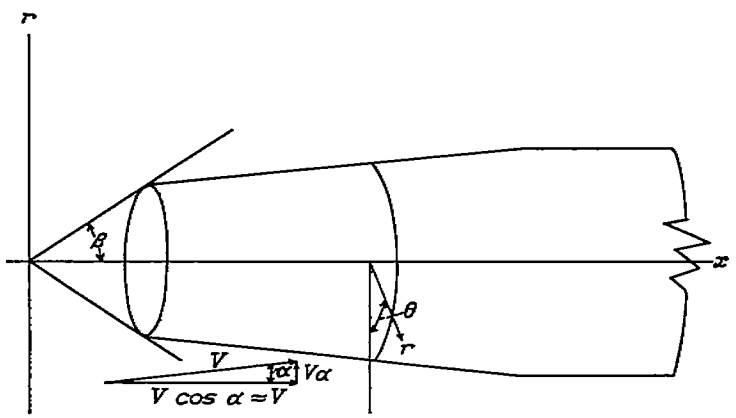

FIGURE 1.—Coordinate system.

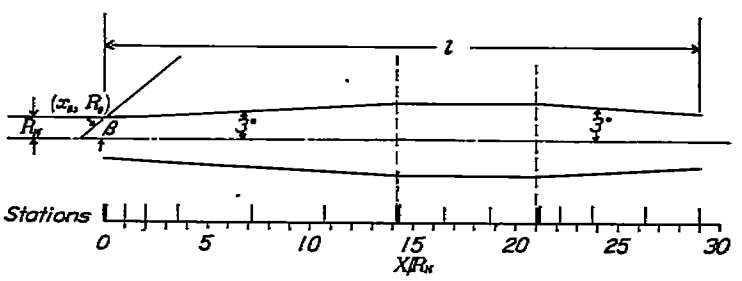

FIGURE 2.—Location of integration stations and intervals on a typical ram-jet body.

By following the method of reference 2, the lift and moment coefficients for small angles of attack based on the area of the nose may be written

$$C_L=-\frac{4}{\pi R_N^2 V}\int_0^{\pi}\int_{BR_N}^{l+BR_N}\frac{\partial\phi_2}{\partial x}\cos\theta\,d\theta\,R\,dx \tag{15}$$

$$C_m=\frac{4}{\pi R_N^2 lV}\int_0^{\pi}\int_{BR_N}^{l+BR_N}\left(x-\frac{l}{2}-BR_N\right)\frac{\partial\phi_2}{\partial x}\cos\theta\,d\theta\,R\,dx \tag{16}$$

where l is the length of the body, R_N is the nose radius, and the moments are taken about the midpoint of the body. By substituting the expression for $\partial\phi_2/\partial x$ in equations (15) and (16), C_L and C_m become

$$C_L=\frac{4B}{\pi R_N^2 V}\int_0^{\pi}\cos^2\theta\,d\theta\int_{BR_N}^{l+BR_N}R\,dx\int_0^{x-BR}\frac{f_2'(\xi)(x-\xi)d\xi}{BR\sqrt{(x-\xi)^2-B^2R^2}} \tag{17}$$

$$C_m=-\frac{4}{\pi R_N^2 Vl}\int_0^{\pi}\cos^2\theta\,d\theta\int_{BR_N}^{l+BR_N}\left(x-\frac{l}{2}-BR\right)R\,dx\int_0^{x-BR}\frac{f_2'(\xi)(x-\xi)d\xi}{BR\sqrt{(x-\xi)^2-B^2R^2}} \tag{18}$$

The distribution function $f_2(\xi)$ must be determined by the boundary condition; thus,

$$V\alpha\cos\theta=\left(\frac{\partial\phi_2}{\partial r}\right)_{r=R} \tag{19}$$

for which the radial velocity is assumed to be normal to the surface. A more rigorous boundary condition taking into account the slope of the body was given by Ferrari (reference 4). For small surface angles, however, equation (19) is within the accuracy of the small-perturbation assumptions. The expression

$$\left(\frac{\partial\phi_2}{\partial r}\right)_{r=R}=\frac{\cos\theta}{R^2}\int_0^{x-BR}\frac{f_2'(\xi)(x-\xi)^2d\xi}{\sqrt{(x-\xi)^2-B^2R^2}} \tag{20}$$

is integrated numerically for constant values of $f_2'(\xi)=K_i$ over the ith interval of integration to obtain the sum

$$\left(\frac{\partial\phi_2}{\partial r}\right)_{r=R}=\frac{B^2\cos\theta}{2}\sum_{i=1}^{n}K_i\left[\cosh^{-1}(T_{i-1}^{\,n})-\cosh^{-1}(T_i^{\,n})+(T_{i-1}^{\,n})\sqrt{(T_{i-1}^{\,n})^2-1}-T_i^{\,n}\sqrt{(T_i^{\,n})^2-1}\right] \tag{21}$$

Substituting this equation in equation (19) gives

$$1=\sum_{i=1}^{n}\frac{B^2K_i}{2V\alpha}\left[\cosh^{-1}(T_{i-1}^{\,n})-\cosh^{-1}(T_i^{\,n})+(T_{i-1}^{\,n})\sqrt{(T_{i-1}^{\,n})^2-1}-T_i^{\,n}\sqrt{(T_i^{\,n})^2-1}\right] \tag{22}$$

With the values of $\frac{B^2K_i}{2V\alpha}$ determined, equations (17) and (18) become

$$C_L=\frac{2\alpha}{R_N^2B}\sum_n(x_n-x_{n-1})(R_n+R_{n-1})\frac{1}{2}\left\{\sum_{i=1}^{n}\frac{B^2K_i}{2\alpha V}\left[\sqrt{(T_{i-1}^{\,n})^2-1}-\sqrt{(T_i^{\,n})^2-1}\right]+\sum_{i=1}^{n-1}\frac{B^2K_i}{2\alpha V}\left[\sqrt{(T_{i-1}^{\,n-1})^2-1}-\sqrt{(T_i^{\,n-1})^2-1}\right]\right\} \tag{23}$$

$$C_m=\frac{2\alpha}{R_N^2Bl}\sum_n\left(\frac{l+2BR_N}{2}-\frac{x_n+x_{n-1}}{2}\right)(x_n-x_{n-1})(R_n+R_{n-1})\frac{1}{2}\left\{\sum_{i=1}^{n}\frac{B^2K_i}{2\alpha V}\left[\sqrt{(T_{i-1}^{\,n})^2-1}-\sqrt{(T_i^{\,n})^2-1}\right]\right.$$
$$\left.+\sum_{i=1}^{n-1}\frac{B^2K_i}{2\alpha V}\left[\sqrt{(T_{i-1}^{\,n-1})^2-1}-\sqrt{(T_i^{\,n-1})^2-1}\right]\right\} \tag{24}$$

In equations (23) and (24) the pressure used for a given integration interval is the average of the pressures at the beginning and at the end of the interval. This scheme of using average lifting pressure is particularly necessary in regions where the pressure is rapidly changing. The method does not give the pressure at the beginning of the first integration interval, that is, at the point $n=0$. It can be shown that, as the first interval approaches zero, the pressure at the lip ($n=0$) is obtained by letting the expression in equations (23) and (24)

$$\sum_{i=1}^{n-1}\frac{B^2K_i}{2\alpha V}\left[\sqrt{(T_{i-1}^{\,n-1})^2-1}-\sqrt{(T_i^{\,n-1})^2-1}\right]$$

have the value 0.5 when $n=1$.

METHOD OF CALCULATION

If calculations are to be made for an open-nose body, the total number of integration stations chosen is a compromise between the amount of labor involved and the accuracy desired, due consideration being given to the limitation on the accuracy imposed by the basic assumptions of small disturbances and potential flow. In general, where the pressures are changing most rapidly the integration stations should be the most dense.

The integration stations must first be chosen. (See fig. 3.)

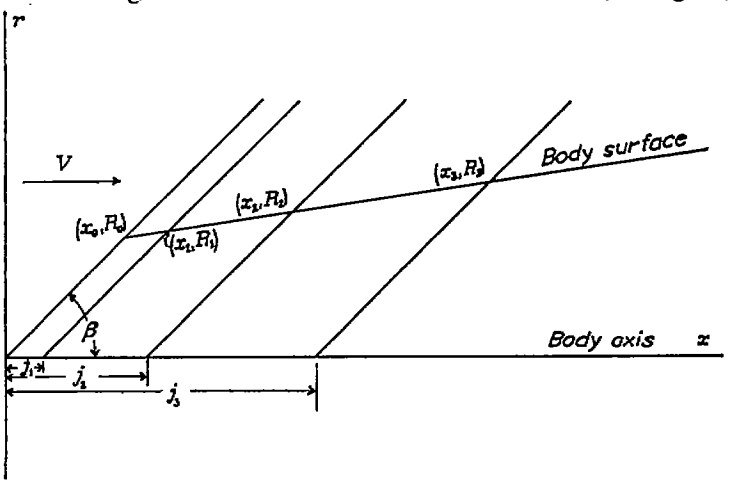

FIGURE 3.—Diagrammatic sketch to illustrate integration process for body selected for calculations.

The calculation for the lift and moment then proceeds as follows:

The boundary condition, equation (22), is applied to the point $n=1$, the summation reducing to a single term, where

$$T_1^1=\frac{x_1-j_1}{BR_1}$$

and

$$T_{1-1}^1=\frac{x_1-0}{BR_1}$$

Equation (22) then gives a value of $B^2K_1/2V\alpha$. Next, equation (22) is applied to point 2, $n=2$, containing now two terms. Substitution of the expressions

$$T_2^2=\frac{x_2-j_2}{BR_2}$$

$$T_1^2=\frac{x_2-j_1}{BR_2}$$

$$T_0^2=\frac{x_2-0}{BR_2}$$

and use of the value obtained for $B^2K_1/2V\alpha$ permits the calculation of the value of $B^2K_2/2V\alpha$.

By continuing the process, at each successive station one more term occurs in equation (22) involving one new K_t, which is then determined. With the values of $B^2K_t/2V\alpha$ determined, equations (23) and (24) are used to evaluate the lift and moment coefficients. It will be noticed that, when equations (23) and (24) are evaluated for $n=1$, the expression occurring after the last summation symbol is unobtainable. For reasons previously stated, the expression must be given the value 0.5.

The procedure for calculating the drag pressures is similar to but somewhat simpler than that for the lift and moment. Equations (4) and (5) are evaluated at the point $n=1$, the sums reducing to one term. By applying the boundary conditions (equation (6)) and using the known slope of the body dr/dx, the constant A_1 occurring in equations (4) and (5) is determined. Substitution of A_1 back into equations (4) and (5) gives the increment velocities at $n=1$. Bernoulli's expression (equation (7)) then gives the pressure ratio at $n=1$. It is to be noted, since $V=Ma$, that actually values of A_1/a, v_{r_1}/a, and v_{x_1}/a are determined. Proceeding to the point $n=2$, one new A is involved in equations (4) and (5) that is determined by the boundary condition in equation (6). In the same way, the velocities and the pressure ratio are calculated at $n=2$. The process is continued at successive integration stations over the whole body. The calculated values of the pressure ratio allow a pressure-distribution curve to be drawn and the drag coefficient to be evaluated in the usual manner.

DISCUSSION OF RESULTS

RESULTS OF CALCULATIONS

Calculations were made in order to obtain the pressure drag, lift, and moment of a typical open-nose body. A sketch showing the dimensions, the integration stations, and intervals is given in figure 2. Calculated pressure distributions at zero angle of attack for the Mach numbers 1.45, 1.60, 1.75, and 3.00 are presented in figure 4. The pressure rise at the nose lip is approximately that which would be obtained over a two-dimensional wedge of the same angle. Ackeret's theory for small disturbances (reference 5) gives for the pressure rise of a 3° wedge $\frac{p_2}{p_1}=1.147$ at $M=1.45$, whereas the pressure ratio on the lip of the open-nose body is about 1.140. This agreement is considered a reasonable check inasmuch as the pressure on the lip must be an extrapolation of the pressure distribution from the first point of the integration process, which must be a finite distance back of the lip edge. It can be shown that, as the size of the first interval approaches zero, the pressure at the lip becomes that given by the two-dimensional theory. The effect over the nose section of the size of integration intervals is illustrated by figure 5. The 17-point method was chosen because a greater number of points resulted in only a small increase in accuracy and a large increase in the labor involved. As would be expected, for the case of the straight conical nose, the pressure falls off from the leading edge and approaches the pressure of a cone of the same surface angle (reference 1). At the corners of the body, the pressure falls approximately in accordance with the Prandtl-Meyer relation (reference 6) for supersonic flow around a two-dimensional corner. On the center and tail sections there are positive pressure gradients that for actual flight conditions would tend to cause separation. The source-distribution functions corresponding to the pressure distributions of figure 4 have been plotted in figure 6.

The incremental surface pressures giving rise to the lift and moment are shown in figure 7 for the Mach numbers 1.60 and 3.00. At the higher Mach numbers the pressures decrease less rapidly over the nose section. The doublet-distribution functions at the four Mach numbers are presented in figure 8. The curves of figure 9 show the theoretical variation of lift-curve slope, moment-curve slope, and drag coefficient with Mach number. The rather interesting result obtained is that the lift coefficient increases with Mach number. Experimental results presented in reference 7 show an increasing lift-curve slope with Mach number for a pointed projectile. The fact that the doublet distribution for the open-nose body is similar to that of a typical projectile (reference 2) leads to the expectation that the Mach number characteristics of the two shapes would be similar. The center of pressure at the lower Mach numbers is ahead of the nose and moves back with increasing Mach number. The drag coefficient can be seen to decrease with Mach number but to a lesser degree than the $\frac{1}{\sqrt{M^2-1}}$ law of two-dimensional wing profiles.

COMPARISON WITH EXPERIMENT

A comparison of the calculated lift and moment coefficients with some experimental data obtained in the Langley 9-inch supersonic tunnel is presented in figures 10(a), 10(b), and 10(c). The contribution to the lift of the internal air can be shown to be:

$$\Delta C_L=2\alpha$$

This increment will appear at the nose and will therefore give rise to a moment:

$$\Delta C_m=\alpha$$

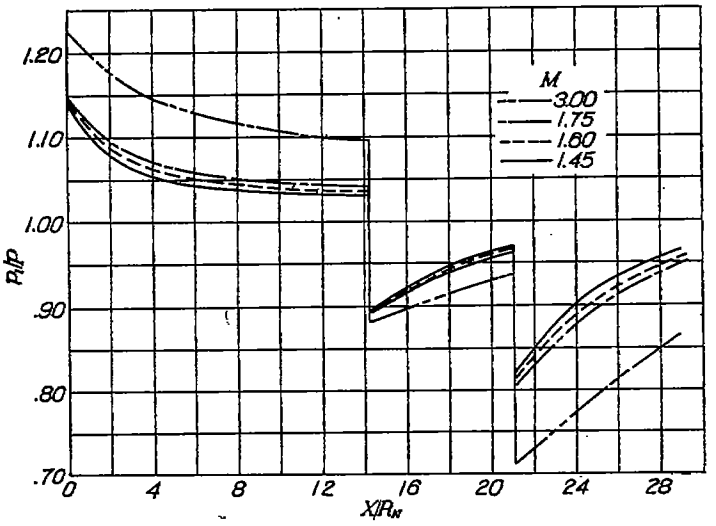

FIGURE 4.—Calculated pressure distributions for $\alpha=0°$

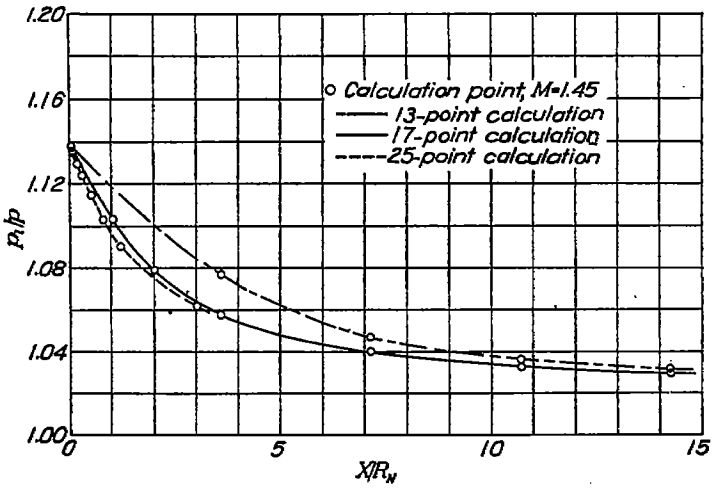

FIGURE 5.—Effect of number of integration points on pressure distribution over the nose of the body

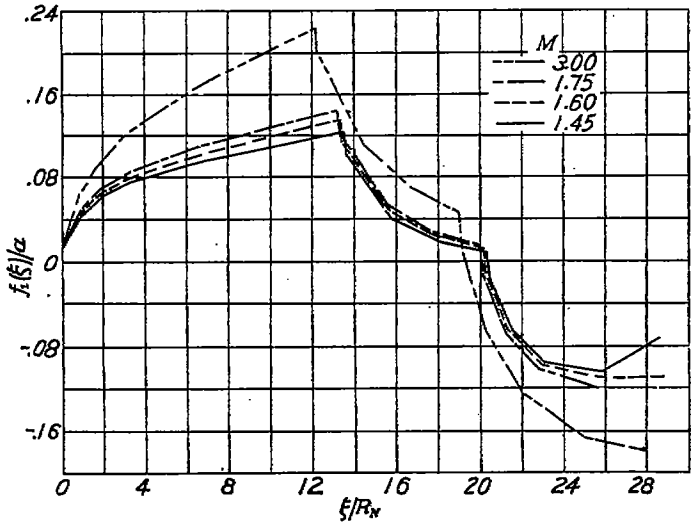

FIGURE 6.—Source-distribution functions for $\alpha=0°$.

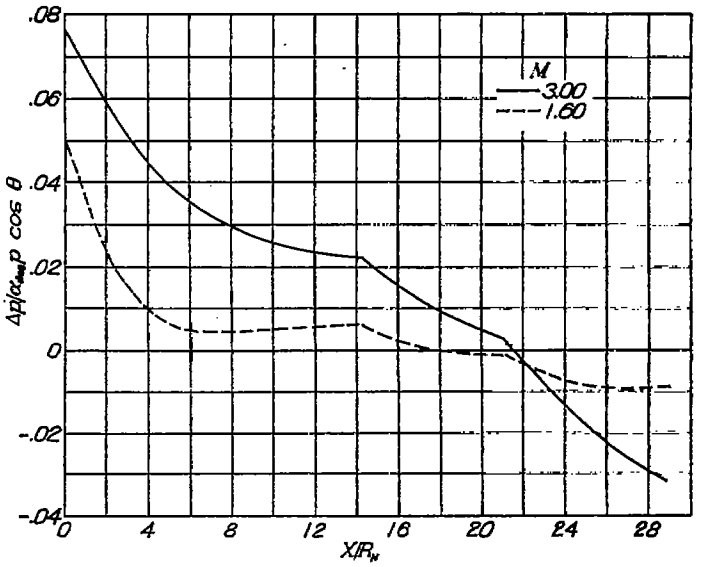

FIGURE 7.—Distribution of incremental surface pressures over the body at two Mach numbers

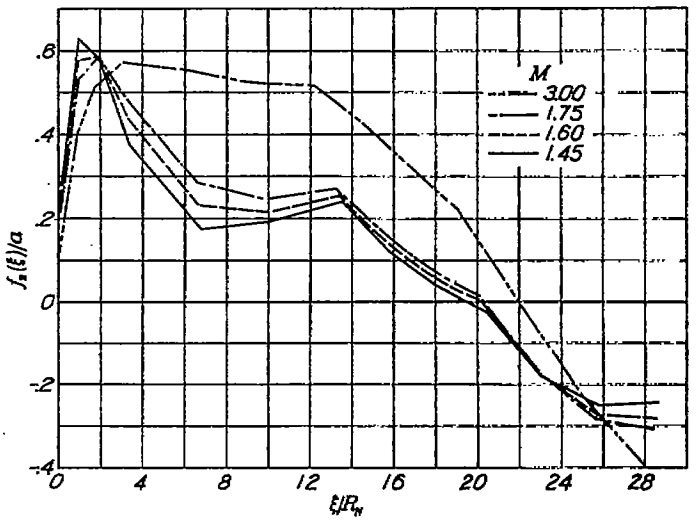

FIGURE 8.—Doublet-distribution functions.

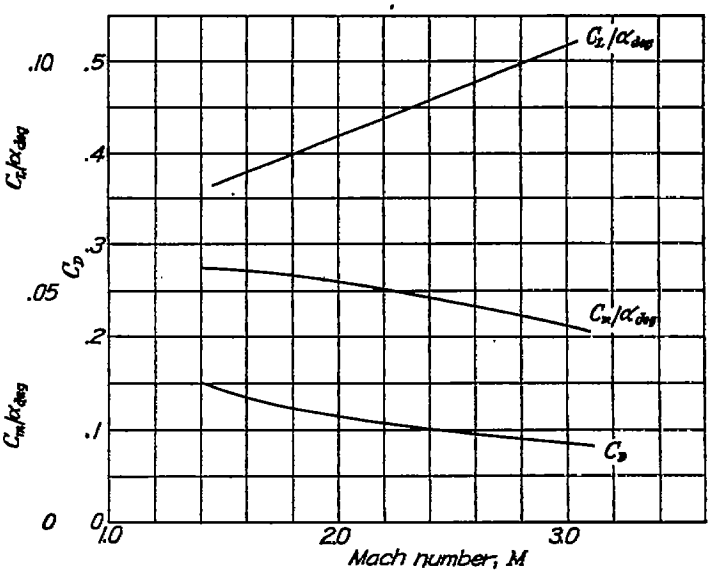

FIGURE 9.—Theoretical variation of lift, moment, and drag coefficients with Mach number.

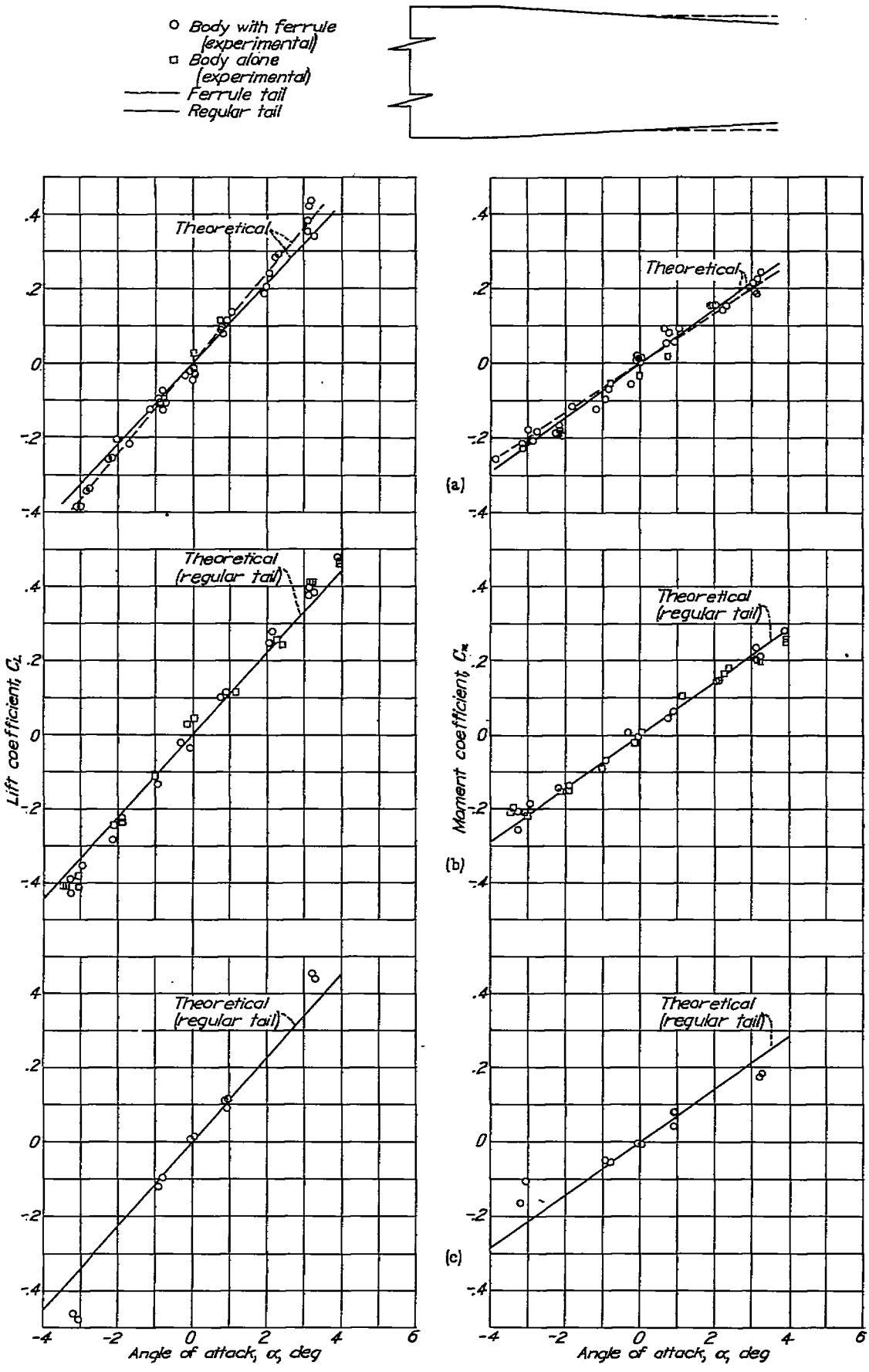

(a) M=1.45.
(b) M=1.60.
(c) M=1.75.

FIGURE 10.—Comparison of calculated lift and moment coefficients with experimental data.

These increments have been added to the calculated results for comparison with the experimental data that include the effect of the internal air. The experimental lift and moment results did not go through the origin because of deviations in the stream flow and perhaps small, unaccounted for, tare forces. It is obvious that for bodies of revolution the data should give symmetrical curves about the origin. The experimental results were therefore made to go through the origin by subtracting from each point the value of the lift coefficient or moment coefficient at zero angle of attack. All coefficients are based on the nose area.

For $M=1.45$ two calculated curves corresponding to two body shapes tested are shown. The two shapes, which are designated for convenience regular tail and ferrule tail, differ only in that a stabilizer-supporting ferrule was placed over part of the tail section. The two configurations are shown in figure 10(a). No difference can be observed in the experimental results for the two shapes, whereas the calculations show a small difference. A possible conclusion is that thickening of the boundary layer ahead of the shock at the trailing edge tends to make the effective shape of the regular body more nearly like that of the body with the tail ferrule. The better agreement of the ferrule-tail calculation is further evidence that this thickening of the boundary layer actually occurs. In any case, the calculated results are in excellent agreement with the experimental data. At $M=1.60$ and $M=1.75$, only the regular shape was calculated, and, although the agreement with the experimental data is good, ferrule-tail calculations would probably have given even better agreement. The discrepancy at $M=1.75$ between the theoretical and experimental points near $\pm 3°$ is probably due to separation phenomena. The agreement is good at small angles of attack. Because of the uncertain value of the skin-friction drag present in the experimental data, a drag comparison is not presented.

ANOTHER APPLICATION

The success of the method when it is applied to open-nose bodies suggests its use in the calculation of external lift, moment, and pressure drag of bodies of revolution having annular air inlets (fig. 11). The characteristics of a body of this type would be calculated as follows: The source and doublet distribution from 0 to B would be numerically determined by the methods of references 1 and 2, which would allow the calculation of the lift, moment, and drag contributions of the portion of the body from 0 to C. In order to calculate the lift, moment, and drag of the remaining external shell, the source and doublet distribution from 0 to A would be retained and a new source and doublet distribution beginning at A and satisfying the boundary condition at the outer shell would be determined. In this way, the influence of the forward portion of the body on the flow along the outer shell would be fully taken into account. The flow at the annular inlet could be fully determined from the original source and doublet distribution from 0 to B, which would allow the determination of the lift due to the internal flow. The moment would be closely approximated by assuming this incremental lift to act at the lip of the inlet.

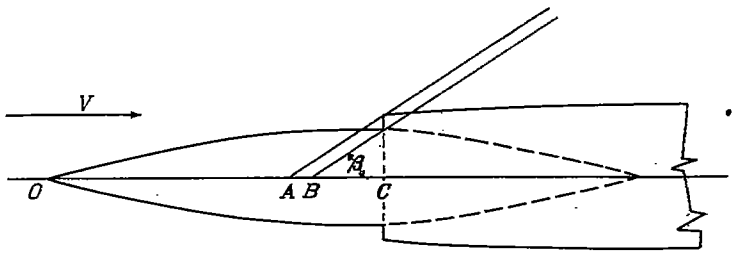

FIGURE 11.—Sketch of a typical body with annular inlet to illustrate the method of calculation.

CONCLUSIONS

An approximate method was presented for the calculation of the external lift, moment, and pressure drag of slender open-nose bodies of revolution at supersonic speeds. The pressure-drag comparison was not presented because of the uncertainty of the amount of skin-friction drag present in experimental results. The calculated lift and moment results at Mach numbers of 1.45, 1.60, 1.75, and 3.00 showed excellent agreement with the available experimental data. The excellent agreement of the calculated lift and moment results with experimental data indicated that the approximate method may be reliably used for obtaining the aerodynamic characteristics of slender bodies that are required for efficient supersonic flight.

LANGLEY MEMORIAL AERONAUTICAL LABORATORY,
NATIONAL ADVISORY COMMITTEE FOR AERONAUTICS,
LANGLEY FIELD, VA., *December 29, 1945.*

REFERENCES

1. Von Kármán, Theodor, and Moore, Norton B.: Resistance of Slender Bodies Moving with Supersonic Velocities, with Special Reference to Projectiles. Trans. A. S. M. E., vol. 54, no. 23, Dec. 15, 1932, pp. 303–310.
2. Tsien, Hsue-Shen: Supersonic Flow over an Inclined Body of Revolution. Jour. Aero. Sci., vol. 5, no. 12, Oct. 1938, pp. 480–483.
3. Lamb, Horace: Hydrodynamics. Sixth ed., Cambridge Univ. Press, 1932, p. 527.
4. Ferrari, C.: Campi di corrente ipersonora attorno a solidi di rivoluzione. L'Aerotecnica, vol. XVII, fasc. 6, June 1937, pp. 507–518.
5. Ackeret, J.: Air Forces on Airfoils Moving Faster Than Sound. NACA TM No. 317, 1925.
6. Taylor, G. I., and Maccoll, J. W.: The Mechanics of Compressible Fluids. Two-Dimensional Flow at Supersonic Speeds. Vol. III of Aerodynamic Theory, div. H, ch. IV, sec. 5, W. F. Durand, ed., Julius Springer (Berlin), 1935, pp. 243–246.
7. Ferri, Antonio: Supersonic-Tunnel Tests of Projectiles in Germany and Italy. NACA ACR No. L5H08, 1945.